Novel Benzo[1,2-*c*]1,2,5-Oxadiazole *N*-Oxide Derivatives as Antichagasic Agents: Chemical and Biological Studies

Claudio Olea-Azar[1,*], Carolina Rigol[1], Fernando Mendizábal[2], Hugo Cerecetto[3,*], Rossanna Di Maio[3], Mercedes González[3], Williams Porcal[3], Antonio Morello[4], Yolanda Repetto[4] and Juan Diego Maya[4]

[1]*Departamento de Química Inorgánica y Analítica, Facultad de Ciencias Químicas y Farmacéuticas, Universidad de Chile*

[2]*Departamento de Química, Facultad de Ciencias Universidad de Chile*

[3]*Departamento de Química Orgánica, Facultad de Química-Facultad de Ciencias, Universidad de la República*

[4]*Programa de Farmacología Molecular y Clínica, Facultad de Medicina, Universidad de Chile*

Received January 01, 2005: Accepted March 07, 2005

Abstract: In order to gain inside the mechanism of action of a series of benzo[1,2-*c*]1,2,5-oxadiazole *N*-oxide derivatives with *in vitro* anti-trypanosomal activity, electrochemical and biological studies were performed. Cyclic voltammetry and electron spin resonance spectroscopy were used to predict the bio-reduction processes. Effects on the parasitic respiration were studied.

Keywords: Benzo[1,2-*c*]1,2,5-oxadiazole *N*-oxide, *Trypanosoma cruzi*, cyclic voltammetry, ESR spectroscopy, cellular respiration.

INTRODUCTION

Trypanosoma cruzi (*T. cruzi*) is the etiologic agent of Chagas' disease. Chagas' disease is mainly a Third World disease that affects approximately 24 million people from Southern California to Argentina and Chile [1], being the current chemotherapy against Chagas' disease still inadequate [2]. Many experiments carried out on the only two drugs commonly used to treat this illness, Nifurtimox (Nfx) and Benznidazole (Bnz) (Fig. **1**), suggest that their intracellular reduction followed by redox cycling yielding $O_2^{-\bullet}$ and eventually $OH^{\bullet}$, may be their major mode of action against *T. cruzi* [3-5].

We have previously reported studies on antiprotozoal 5-nitrofurfural and 5-nitrothiophene-2-carboxaldehyde derivatives [6]. These compounds were capable to generate nitro anion radical chemically and biologically, which were characterized using electron spin resonance (ESR) spectroscopy [7]. Like the nitro pharmacophore of antitrypanosomal drugs, the *N*-oxide moiety has proved to be responsible for the biological activity of different drug families, with antitumor or antibacterial activities, through the production of free radical species [8,9].

Recently, we have reported on the 1,2,5-oxadiazole *N*-oxide family in order to determine their antitrypanosomal behavior testing *in vitro* against the epimastigote form of *T. cruzi*. These new structures were based on the conjunction of different *N*-oxide systems and "spermidine- mimetic" lateral chains [10]. The spermidine-mimetic lateral chain did not improve the activity, however, the *N*-oxide moiety resulted very important for the activity of these compounds. Moreover, we have electrochemically shown the facile electroreduction of the *N*-oxide moiety and also have characterized the free radical species generated by microsomal reduction using ESR spectroscopy [10,11]. Further, these results allowed us to select benzo[1,2-*c*]1,2,5-oxadiazole *N*-oxide (benzofuroxan) system as template for further chemical modifications [12], resulting in derivative **1** (Fig. **1**) as a new benzofuroxan anti-trypanosomal leader. We found that the lipophilic characteristics of these new analogs were related to activity. The ESR spectra of the radical of derivative **2** (Fig. **1**) generated *in vitro* with *T. cruzi*, when 5,5-dimethyl-1-pyrroline *N*-oxide (DMPO) was added to the system, were consistent with the trapping of the *N*-oxide radical [13]. Biological studies and *T. cruzi*-ESR experiments indicated that **2** did not act by production of oxidative stress.

Based on compound **1** which exhibited excellent anti-trypanosomal activity, we have developed new benzofuroxans related to this compound that did not include the semicarbazide moiety like **2** (Fig. **1**). Herein, we report the synthesis, the biological characterization and the electrochemical studies of these new *N*-oxide derivatives. The anion radicals produced electrochemically were characterized by ESR spectroscopy and the corresponding hyperfine constants were theoretically determined. In order to know the relationship between benzofuroxans free-radical release capacities and *in vitro* anti-trypanosomal activities, the effect of new compounds in the *T. cruzi* respiration and parasite toxicity was studied.

*Address correspondence to this author at these Departamento de Química Inorgánica y Analítica, Facultad de Ciencias Químicas y Farmacéuticas, Universidad de Chile, Casilla 233, Santiago 1, Chile; Tel: +56-26782846; Fax: +56-2-7370567; E-mail: colea@uchile.cl; Laboratorio de Química Orgánica, Facultad de Ciencias, Universidad de la República, Iguá 422, 11400 Montevideo, Uruguay; Tel: +598 2 525 86 18 (ext. 216); Fax: +598 2 525 07 49; E-mail: hcerecet@fq.edu.uy

1570-1808/05 $50.00+.00

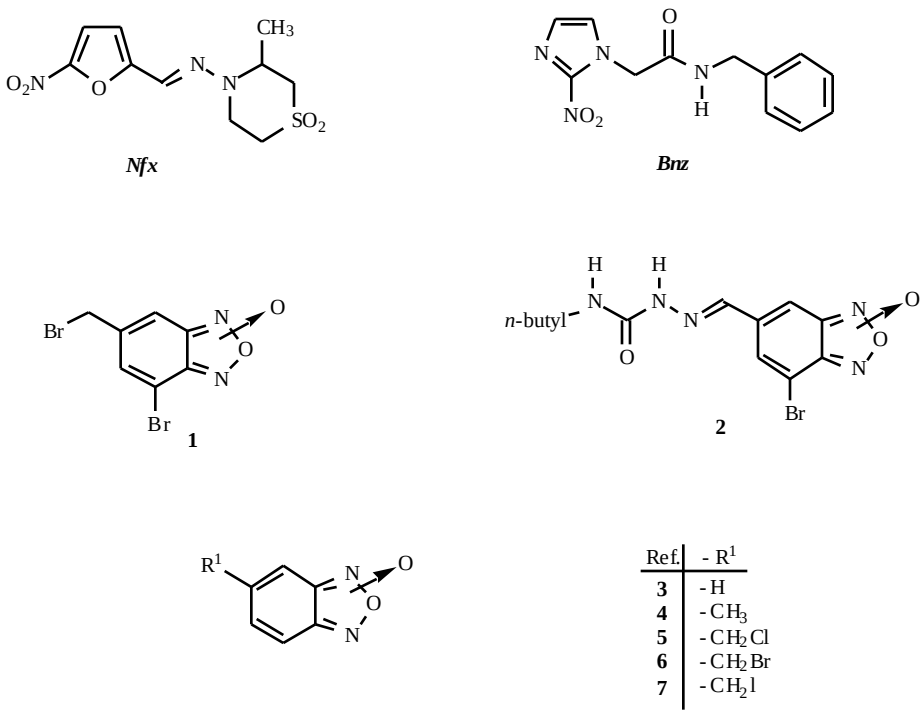

Fig. (1). Nfx, Bnz and benzofuroxan derivatives.

RESULTS AND DISCUSSION

Chemistry

The *N*-oxide without the lateral chain and the halogen, derivatives **3** and **4** (Fig. **1**), were prepared according to literature [12,14]. The halo derivatives, **5-7** (Fig. **1**), were prepared in moderate yields as is depicted in Scheme **1**. The benzofuroxan derivatives exist as a mixture of isomers at room temperature (**A** and **B**, Fig. **2a**). At room temperature (303 K), ^{1}H and ^{13}C NMR spectra of the benzofuroxans show benzo-protons and -carbons as broad peaks, indicating extensive benzofuroxan tautomerism [15]. On cooling, the broad signals were resolved below 263 K, making possible the record of the complete series of spectra (^{1}H, ^{13}C NMR, and HMQC, and HMBC experiments), as it is shown by the spectrum of compound **5** displayed in (Fig. **2b-c**). In $CDCl_3$ solution (approximately 10 % w/v) at 303 K, compound **5** shows a 400 MHz ^{1}H and a 100 MHz ^{13}C NMR spectra with broad resonance signals due to incomplete coalescence (Fig. **2b**); on cooling, the broad signals were resolved (Fig. **2c**).

All new compounds were identified by IR, MS, ^{1}H NMR, ^{13}C NMR, and HETCOR experiments, and their purity was established by TLC and microanalysis.

Biological Activity in *T. cruzi* Parasites

Table 1 shows the effect of benzofuroxan derivatives on the growth and respiration of *T. cruzi* epimastigotes (see Experimental Section for experimental details and definitions). The growth inhibition is expressed as $ICkc_{50}$. Derivative **5** resulted in the most active compound with an IC_{kc50} of 5.7 μM. Compounds **6** and **7** showed an $ICkc_{50}$ close to 10 μM. Besides, Nfx inhibitory concentration resulted close to 15 μM. The MTT assays [16] showed that derivatives **5-7** proved more toxic against the parasite than

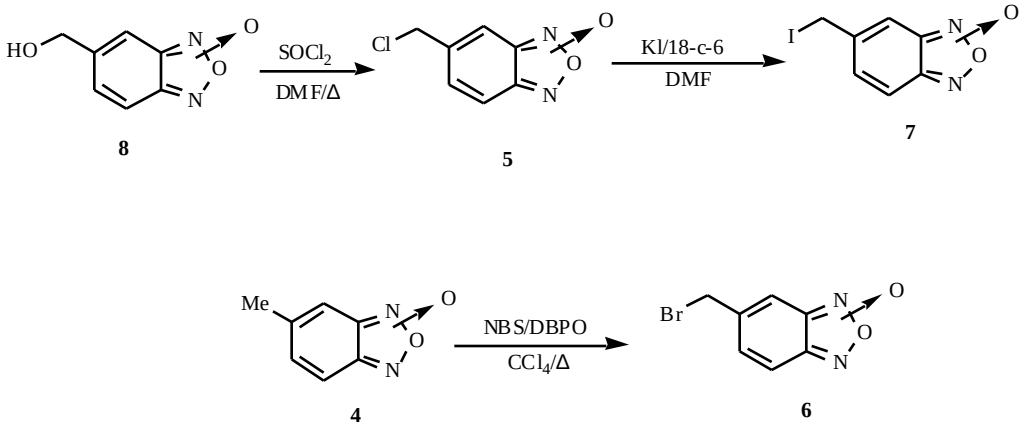

Scheme 1. Benzofuroxans synthetic procedures.

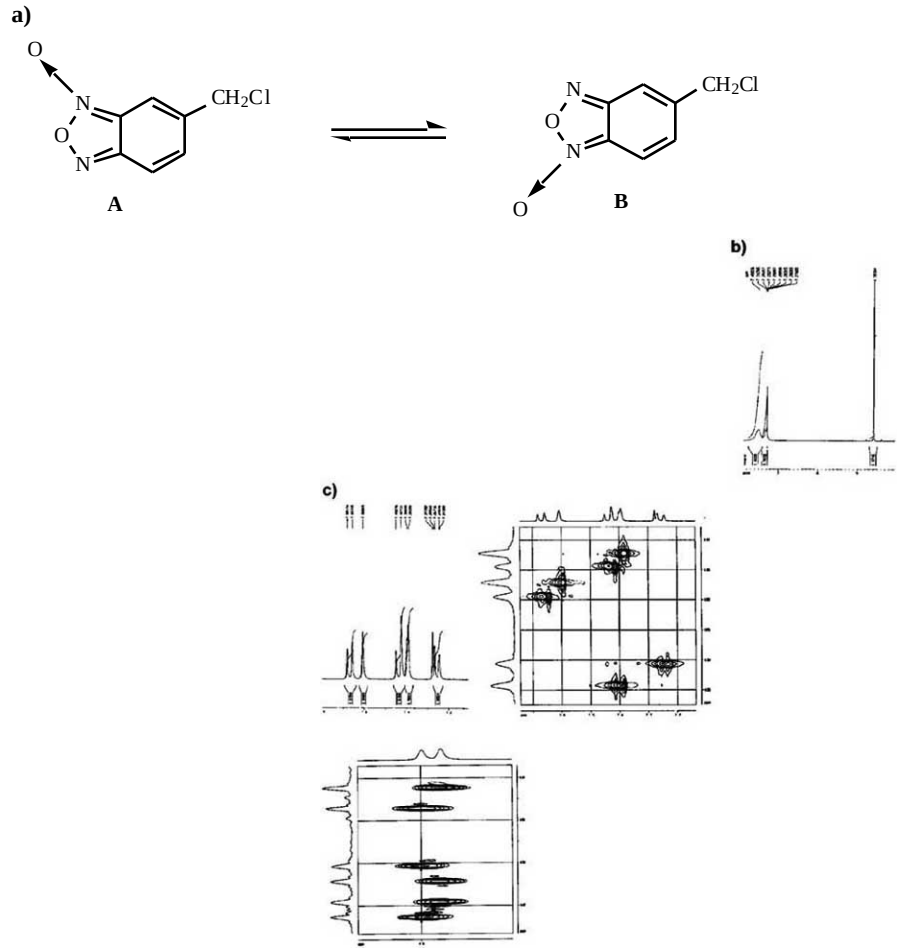

Fig. (2). a) Derivative **5** tautomeric equilibrium at room temperature. **b**) ^{1}H NMR spectra of **5**, in $CDCl_3$, at 303 K. c) Selected region of ^{1}H NMR, HMQC, and HMBC spectra of **5**, in $CDCl_3$, at 243 K.

Nfx. Otherwise, benzofuroxans **3** and **4** possess the same or less cytotoxic effects than the referenced drug Nfx. Table 1 also shows the inhibition of *T. cruzi* epimastigote respiration by these compounds. Derivative **7** inhibited the cellular respiration, whereas the other derivatives promoted an oxygen consumption similar to that of control. Perhaps, for the active derivatives **5** and **6**, the same degree of oxygen consumption as the control could be the result of an oxidative stress process promoted from them.

Cyclic Voltammetry

The electrochemical studies of benzofuroxan derivatives in dimethylsulfoxide (DMSO) were performed using cyclic

Table 1. Effect of Benzofuroxan Derivatives Upon Growth and Oxygen Uptake of *T. cruzi*

Derivative	IC_{kc50} [a,b] (μM)	Viable parasites (% of control)[b,c]	Respiration[d]	
			nanoatom of oxygen/min/mg protein[b]	% of control
3	30.8 ± 0.5	27.6 ± 6.7	17.3 ± 1.2	88.7
4	36 ± 5	40.2 ± 0.2	17.1 ± 0.8	87.7
5	5.7 ± 0.1	21.3 ± 0.9	19.5 ± 0.9	100
6	10.8 ± 0.3	19.3 ± 0.4	17.9 ± 0.4	91.8
7	10.2 ± 0.1	13.4 ± 0.2	9.8 ± 0.5	50.3
Nfx	14.91 ± 0.05	26.5 ± 0.4	23.0 ± 1.0	118.2

a.IC_{kc50} is the drug concentration needed to diminish the control growth kc in 50%. Further details are described in Experimental Section.
b.All experiments represent average ± SD of at least three independent experiments.
c.Cytotoxicity assays were performed with the MTT reduction method [16]. Controls without drugs correspond to 100% of viable parasites. See Experimental Section.
d.T. cruzi epimastigote respiration values are expressed as nanoatom of oxygen consumed during one minute per mg of protein and as % of control (control respiration 19.5 ± 1.5 nanoatom of oxygen/min/mg protein).

voltammetry experiments. These *N*-oxides displayed comparable voltammetric behavior in DMSO, showing two well-defined reduction waves (see example in Fig. **3**). The first wave corresponds to a quasireversible process. We have studied the stability of the species generated by changing the electrochemical conditions, *i.e.* the scan rate and the switching potential, while keeping the chemical conditions of the solution constant. Results showed that as the scan rate increases, the ipa/ipc ratio increases, typical for a reversible chemical reaction following a reversible charge transfer [17]. The second cathodic peak is irreversible in the whole range of sweep rates studied (50-2000mV/s). We can attribute this wave to the production of further reduction product, these electrochemical and chemical reactions are summarized in the speculative mechanism showed in (Fig. **4**). Table 2 lists the values of the voltammetric peaks and the anodic and cathodic currents for the five compounds studied. The formal one-electron transfer potential ($E_{1/2}$) for these compounds was compared with that of Nfx. These *N*-oxides showed higher first wave $E_{1/2}$ than Nfx (-0.880 V) [7,11]. Benzofuroxans Epc and $E_{1/2}$ were found dependent on the benzo-substituent electronic characteristics, electron withdrawing substituents (like -CH_2-halogen) presented the lowest Epc and $E_{1/2}$ values.

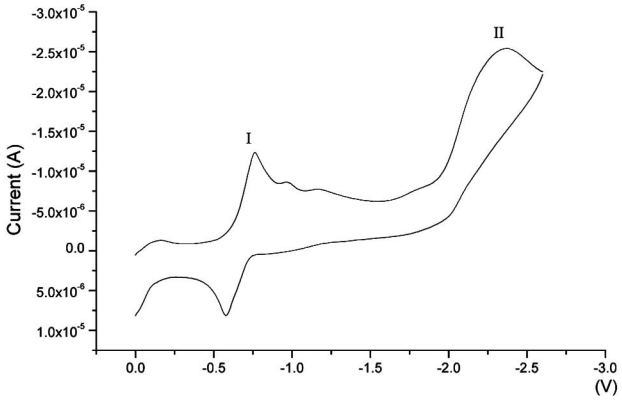

Fig. (3). Voltammogram of derivative **5** in DMSO at room temperature (sweep rate 2000 mV/s).

Except for derivative **4**, the corresponding Epc was higher than first wave Epc_{Nfx} showing that the benzofuroxans derivatives could be easily bio-reduced than Nfx. Clearly, the first reduction potentials (Epc) of compounds **3-7** and Nfx are related to their anti-*T. cruzi* activity. So, benzofuroxans IC_{kc50} resulted lineally related to Epc (r= -0.9301, s= 5.81, p= 0.022) while when we included Nfx into the analysis the quality of statistic parameters decreased (r= -0.7903, s= 8.45, p= 0.061). Besides, viable *T. cruzi* parasites resulted lineally related to Epc (benzofuroxans derivatives and Nfx, r= -0.8427, s= 5.52, p= 0.035; benzofuroxans derivatives, r= -0.8849, s= 5.49, p= 0.046). Similar results were obtained when $E_{1/2}$ was studied instead of Epc.

Electron Spin Resonance

The reduction processes were studied using ESR spectroscopy. The *N*-oxide free radicals were prepared *in situ* by electrochemical reductions in DMSO, applying the potential corresponding to the first wave for the *N*-oxides as obtained from the cyclic voltammetric experiments. The interpretation of the ESR spectra by means of a simulation process led to the determination of the coupling constants for all the magnetic nuclei (Table 3). For derivative **3** the theoretical simulation of the hyperfine pattern was performed using B3LYP/6-31G* calculations on *ab-initio* 3-21G optimized geometry. These hyperfine splitting constants are listed in Table 3. Derivative **3** was analyzed and simulated as two triplets due to the nitrogen atoms of the oxadiazole ring and four doublets assigned to the benzo-ring hydrogen atoms. Derivative **4** showed one broad ESR line. Derivative **5** was analyzed and simulated as two triplets (oxadiazole nitrogen atoms), two doublets (benzo hydrogen atoms) and one quartet due to the chlorine atom. Derivative **6**, like derivative **5**, was analyzed and simulated as two triplets (oxadiazole nitrogen atoms), three doublets (benzo hydrogen atoms) and one quartet (bromine atom) (Fig. **5a**). Derivative **7** was analyzed and simulated as two triplets (oxadiazole nitrogen atoms), two doublets (benzo hydrogen atoms) and one sextuplet (iodine atom) (Fig. **5b**). The hyperfine constant of hydrogen atom 2 (according to structure in Table 3) had the same order of width line as of derivative **5**. The hyperfine constants indicated an excellent delocalization of the electron in the heterocycle system.

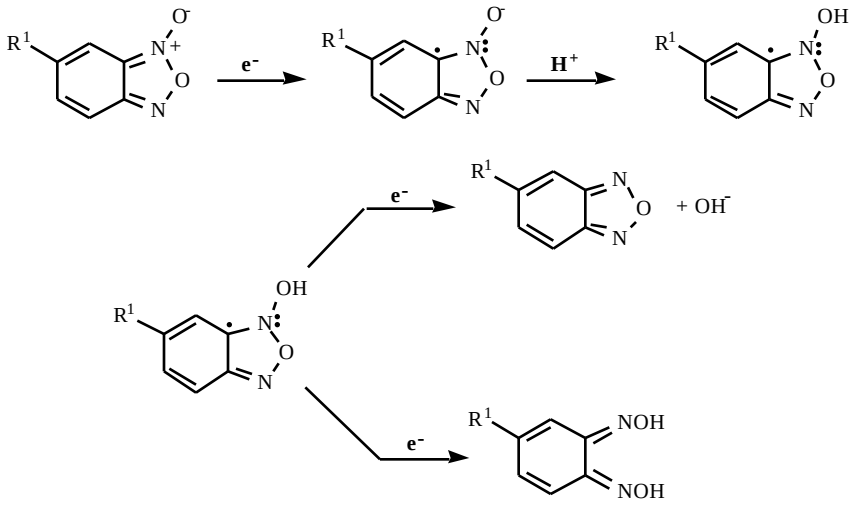

Fig. (4). Speculative reduction mechanism for *N*-oxide derivatives.

Table 2. Cyclic Voltammetric Parameters of *N*-oxide Derivatives *vs.* Saturated Calomel Electrode

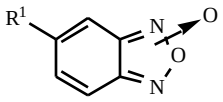

R^1		Epc (V)	Epa (V)	ΔE (V)	ipa/ipc[a]	$E_{1/2}$ (V)
-H	I	-0.898	-0.598	0.30	1.02	-0.748
	II	-2.414	-2.042	0.37	0.50	-2.228
$-CH_3$	I	-0.938	-0.557	0.38	1.31	-0.748
	II	-2.119	-2.006	0.11	0.50	-2.063
$-CH_2Cl$	I	-0.755	-0.583	0.17	1.09	-0.669
	II	-2.419	-1.968	0.45	0.67	-2.194
$-CH_2Br$	I	-0.678	-0.621	0.06	2.58	-0.650
	II	-2.379	-	-	-	-
$-CH_2I$	I	-0.724	-0.633	0.09	2.08	-0.679
	II	-2.400	-1.990	0.41	0.71	-2.195
Nfx	b	-0.910	-0.850	**0.06**	**1.01**	-0.880

a. Sweep rate: 2000 mV/s.
b. Corresponding to nitro reduction peak (Ref. [7a]).

CONCLUDING REMARKS

The newly developed benzofuroxans presented excellent anti-*T. cruzi* activities. Derivatives **5-7** presented lower IC_{kc50} than Nfx with low viable parasites number. Only derivative **7** inhibited the cellular respiration in the assayed conditions while the other halo derivatives, **5** and **6**, could participate in an oxidative stress process. Relationship between activity (as IC_{kc50} or viable cells) and the inhibition of *T. cruzi* respiration was not observed.

The results obtained from the electrochemical studies showed a two-step reduction mechanism for the benzofuroxan derivatives. The first wave was assigned to the generation of the corresponding free radical species, identified by ESR spectroscopy, and the second wave was assigned to the reduction of the oxadiazole heterocyclic system. The *N*-oxide derivatives studied showed lower $E_{1/2}$ than Nfx. Also, the benzofuroxan side chains assessed in this work modified the $E_{1/2}$, an aspect which might be important for the selectivity of these compounds toward *T. cruzi* antioxidant defenses (such as trypanothione reductase [18]). Stable free radicals were obtained using electrochemical reduction at the corresponding first wave potentials from cyclic voltammetry experiments. The hyperfine patterns for all derivatives indicated that the spin electron density is typically delocalized in all the molecule. The electrochemical and ESR studies showed that the observed activities could be associated with the facile monoelectronation of the *N*-oxide moiety.

Table 3. Experimental and Theoretical Hyperfine Splitting (Gauss) and g Values for the *N*-oxide Anion Radicals Studied in DMSO

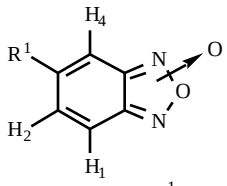

$R^1 = H_3$ or CH_2X (X = H, Cl, Br, I)

Derivative		a_{H1}	a_{H2}	a_{H3}	a_{H4}	a_{N1}	a_{N2}	a_X	g value
		[G]							
3	EXP	4.20	2.60	2.00	3.20	4.70	2.70	-	2.0056
	DFT	3.90	2.25	1.89	2.90	4.30	2.40		
4	EXP	One broad line						-	2.0063
5	EXP	6.95	-	-	3.25	2.10	1.45	3.00	2.0060
6	EXP	3.65	0.40	-	3.05	2.00	1.00	4.60	2.0059
7	EXP	2.75	-		2.60	1.45	0.86	3.83	2.0060

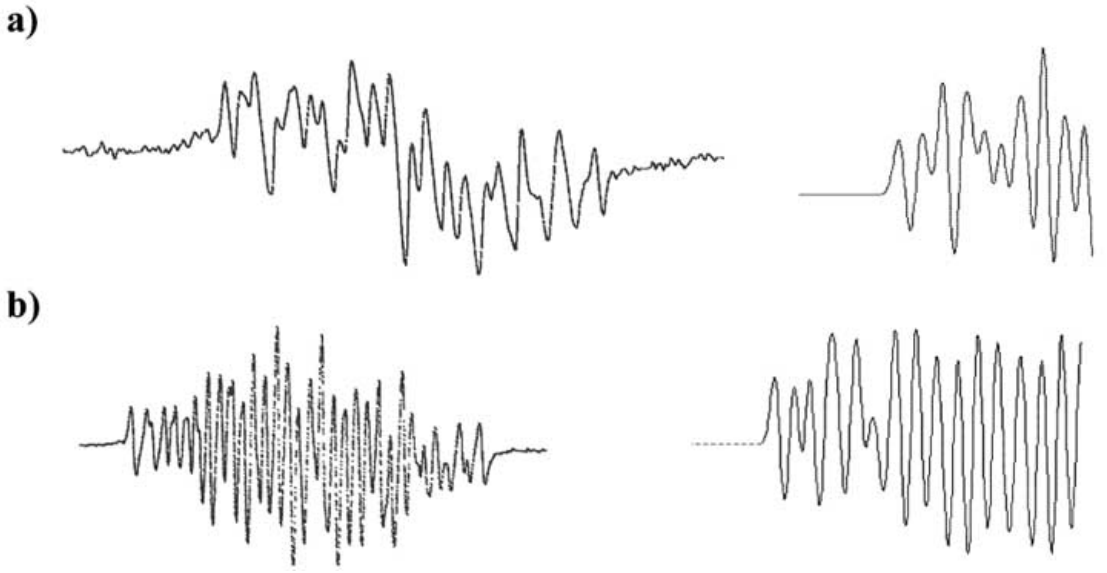

Fig. (5). a) ESR spectra of derivative **6** generated by electrochemical reduction in DMSO (left) and computer simulations of the same spectra (right). **b**) ESR spectra of derivatives **7** generated by electrochemical reduction in DMSO (left) and computer simulations of the same spectra (right).

EXPERIMENTAL SECTION

Chemistry

All starting materials were commercially available research-grade chemicals and used without further purification. Compound **8** and derivatives **3** and **4** were prepared according to literature [10,12,14]. All solvents were dried and distilled prior to use. All the reactions were carried out in a nitrogen atmosphere. Elemental analyses were obtained from vacuum-dried samples (over phosphorous pentoxide at 3-4 mm Hg, 24 h at room temperature) and performed on a Fisons EA 1108 CHNS-O analyzer, and were within ± 0.4 % of theoretical values. Infrared spectra were recorded on a Perkin Elmer 1310 apparatus, using potassium bromide tablets, the frequencies are expressed in cm^{-1}. ^1H NMR and ^{13}C NMR spectra were recorded on a Bruker DPX-400 (at 400 MHz and 100 MHz) instrument, with tetramethylsilane as the internal reference and in the indicated solvent, the chemical shifts are reported in ppm. The ^1H NMR signals reported were obtained at room temperature. Bruker softwares were used to perform HMQC, and HMBC experiments. Mass spectra were recorded on a Shimadzu GC-MS QP 1100 EX instrument, for electronic impact at 70 eV.

5-Chloromethylbenzo[1,2-*c*]1,2,5-oxadiazole *N*-oxide (5): a mixture of alcohol **8** (1.0 g, 6.0 mmol), $SOCl_2$ (1.3 mL, 18 mmol), and DMF (0.15 mL) was heated at reflux during 3 hours. The mixture was neutralized with aqueous $NaHCO_3$ (5 %) and extracted with EtOAc (3x20 mL). The organic layer was dried with sodium sulphate and evaporated *in vacuo*. The crude was purified by column chromatography (SiO_2, petroleum ether:EtOAc (9:1)). Beige oil (0.44 g, 40%). ^1H-NMR ($CDCl_3$, 400 MHz) δ: 4.58 (s, 2H), 7.31 (bs, 1H), 7.49 (bs, 2H). IR ν: 1624, 1583, 1537, 1487. MS *m/z*: 184/186 ($M^{\cdot+}$), 168, 149, 133. Found: C, 45.4; H, 2.70; N, 15.3. $C_7H_5ClN_2O_2$ requires C, 45.6; H, 2.73; N, 15.2.

5-Bromomethylbenzo[1,2-*c*]1,2,5-oxadiazole *N*-oxide (6): a mixture of derivative **4** (0.31 g, 2.0 mmol), *N*-bromosuccinimide (0.38 g, 2.0 mmol), dibenzoylperoxide (0.06 g, 0.2 mmol) and CCl_4 (5.0 mL) was heated at reflux during 72 hours. Then, water (10.0 mL) was added and extracted with EtOAc (3x20 mL). The organic layer was dried with sodium sulphate and evaporated *in vacuo*. The crude was purified by column chromatography (SiO_2, petroleum ether:EtOAc (95:5)). Transparent oil (0.15 g, 32%). ^1H-NMR ($CDCl_3$, 400 MHz) δ: 4.45 (s, 2H), 7.46 (bs, 3H). MS *m/z*: 228/230 ($M^{\cdot+}$), 149, 133. Found: C, 36.5; H, 2.33; N, 12.1. $C_7H_5BrN_2O_2$ requires C, 36.7; H, 2.20; N, 12.2.

5-Iodomethylbenzo[1,2-*c*]1,2,5-oxadiazole *N*-oxide (7): a mixture of derivative **5** (0.1 g, 0.54 mmol), KI (0.45 g, 2.7 mmol), 18-crown-6 (0.68 g, 2.7 mmol), and DMF (2.0 mL) was stirred at room temperature during 4 hours. Then, water (20.0 mL) was added and extracted with EtOAc (3x20 mL). The organic layer was dried with sodium sulphate and evaporated *in vacuo*. The crude was purified by column chromatography (SiO_2, petroleum ether:EtOAc (95:5)). Transparent oil was crystallized at 4 ºC (45 mg, 30 %). ^1H-NMR ($CDCl_3$, 400 MHz) δ: 4.40 (s, 2H), 7.50 (bs, 3H). IR ν: 1620, 1593, 1537, 1480. MS *m/z*: 276 ($M^{\cdot+}$), 149, 133, 89. Found: C, 30.5; H, 1.79; N, 10.0. $C_7H_5IN_2O_2$ requires C, 30.5; H, 1.83; N, 10.1.

Biology

Parasites. T. cruzi epimastigotes (Tulahuen strain), from our collection, were grown at 28 ºC in Diamond's monophasic medium as reported earlier [19], with blood replaced by 4 μM hemin. Fetal calf serum was added to a final concentration of 4%. Parasites: $80x10^6$ cells correspond to 1 mg protein or 12 mg of fresh weight.

Epimastigote Growth Inhibition

Four to five different concentrations of each compound dissolved in DMSO were added to a suspension of $3x10^6$ *T. cruzi* epimastigotes/mL. Parasite growth was followed by nephelometry for 10 days. No toxic effect of DMSO alone was observed. The growth constant (kc) for each compound

concentration employed and the control was calculated using the epimastigotes exponential growth curve (regression coefficient >0.97, p<0.05). The slope resulting from plotting Ln of nephelometry lecture versus time, corresponds to the kc (h^{-1}). ICkc50 is defined as the compound concentration needed to diminish the control growth kc in 50%, calculated by lineal regression analysis from the kc values at the employed concentrations [19b].

Cytotoxicity Assays

These experiments were performed with the MTT reduction method as described previously [16]. Briefly, 3 x 10^6 epimastigotes/mL were incubated with the different *N*-oxide derivatives at the IC_{kc50} concentration during 48 hours in Diamond's culture media at 28 ºC. An aliquot of the parasite suspension was extracted and incubated in a 96-flat bottom well plate and MTT was added at 0.5 mg/mL final concentration, incubated at 28 ºC during 4 hours and then dissolved with 10 % SDS 0.1 mM HCl and incubated over night. The formazan formation was measured at 570 nm in a multiwell reader (Labsystems multiskan MS).

Respiration

The parasites were harvested at the fourth or fifth day of growth by centrifugation at 500g for 10 min, then washed and resuspended with 0.05 M potassium phosphate buffer, pH 7.4, containing 0.107 M sodium chloride. Respiration measurements were carried out polarographically with a Clark Nº 5331 electrode (Yellow Spring Instruments) in a Gilson 5/6 oxygraph [19b]. The chamber volume was 2 mL and the temperature was 28ºC. The amount of parasites used for the assays was equivalent to 2 mg of protein. Drugs were added in DMSO at the IC_{kc50} concentration expressed in nmol of drug/mg protein [19a]. Control respiration was 19.5±1.5 nanoatom of oxygen consumed during one minute per mg of protein. Values are expressed as the mean ± SD of three or more independent experiments.

Cyclic Voltammetry

DMSO (spectroscopy grade) was obtained from Aldrich. Tetrabutylammonium perchlorate (TBAP) used as supporting electrolyte was obtained from Fluka. Cyclic voltammetry was carried out using a Weenking POS 88 instrument with a Kipp Zenen BD93 recorder, in DMSO (*ca* 1.0 x 10^{-3} mol dm^{-3}), under a nitrogen atmosphere, with TBAP (*ca* 0.1 mol dm^{-3}), using three-electrode cells. A mercury-dropping electrode was used as the working electrode, a platinum wire as the auxiliary electrode, and saturated calomel as the reference electrode.

ESR Spectroscopy

The *N*-oxide radicals were generated by electrolytic reduction *in situ* at room temperature. ESR spectra were recorded in the X band (9.85 GHz) using a Bruker ECS 106 spectrometer with a rectangular cavity and 50 kHz field modulation. The hyperfine splitting constants were estimated to be accurate within 0.05 G.

Theoretical Calculations

Full geometry optimization of compound **3** in spin-paired and free radical forms was carried out by *ab-initio* 3-21G* method. The theoretic hyperfine constants were obtained using DFT level (B3LYP/6-31G*) [20].

ACKNOWLEDGEMENTS

This research was supported by FONDECYT 1000834, 7040037, 1020095, CSIC (UdelaR), CLEMENTE ESTABLE and TWAS grants. We thank a scholarship for C. Rigol from RELACQ.

REFERENCES

[1] a) Schofield, C.J. *Br. Med. Bull.*, **1985**, *41*, 187-194.; (b) http://www.who.int/whr/2001.

[2] Cerecetto, H.; González, M. *Curr. Topics Med. Chem.*, **2002**, *2*, 1185-1211.

[3] Hazra, B.; Sur, P.; Sur, B.; Banerjee, A.; Roy, D.K. *Planta Med.*, **1984**, *51*, 295-297.

[4] Docampo, R.; Moreno, S.N.J. *Rev. Infect. Dis.*, **1984**, *6*, 223-238.

[5] Morello, A.; Pavani, M.; Garbarino, J.A.; Chamy, M.C.; Frey, C.; Mancilla, J.; Guerrero, A.; Repetto Y.; Ferreira, J. *Comp. Biochem. Physiol.*, **1995**, *112C*, 119-125.

[6] (a) Cerecetto, H.; Di Maio, R.; Ibarruri, G.; Seoane, G.; Denicola, A.; Peluffo, G.; Quijano, C.; Paulino, M. *Il Farmaco*, **1998** , *53*, 89-94.; (b) Cerecetto, H.; Di Maio, R.; González, M.; Risso, M.; Sagrera, G.; Seoane, G.; Denicola, A.; Peluffo, G.; Quijano, C.; Basombrío, M. A.; Stoppani, A. O. M.; Paulino, M.; Olea-Azar, C. *Eur. J. Med. Chem.*, **2000**, *35*, 343-350.; (c) Martínez-Merino, V.; Cerecetto, H. *Bioorg. Med. Chem.*, **2001**, *9*, 1025-1030.; (d) Paulino, M.; Iribarne, F.; Hansz, M.; Vega, M.; Seoane, G.; Cerecetto, H.; Di Maio, R.; Caracelli, I.; Zukerman-Schpector, J.; Olea, C.; Stoppani, A.O.M.; Berriman, M.; Fairlamb, A.H.; Tapia, O. *J. Mol. Struc.-Theochem.*, **2002**, *584*, 95-105.; (e) Cerecetto, H.; Di Maio, R.; González, M.; Seoane, G.; Duffaut, A.; Denicola, A.; Gil, M. J.; Martínez-Merino, V. *Eur. J. Med Chem.*, **2004**, *39*, 421-431.; (f) Aguirre, G.; Boiani, L.; Cerecetto, H.; Fernández, M.; González, M.; Denicola, A.; Otero, L.; Gambino, D.; Rigol, C.; Olea-Azar, C.; Faúndez, M. *Bioorg. Med. Chem.*, **2004**, 12, 4885-4893.

[7] (a) Olea-Azar, C.; Atria, A.M.; Di Maio, R.; Seoane, G.; Cerecetto, H. *Spectrosc. Let.*, **1998**, *31*, 849-857.; (b) Olea-Azar, C.; Atria, A.M.; Mendizabal, F.; Di Maio, R.; Seoane, G.; Cerecetto, H. *Spectrosc. Let.*, **1998**, *31*, 99-109.; (c) Olea-Azar, C.; Rigol, C.; Mendizabal, F.; Morello, A.; Maya, J. D.; Moncada, C.; Cabrera, E.; Di Maio, R.; González, M.; Cerecetto, H. *Free Rad. Res.* **2003**, *37*, 993-1001.

[8] Cahill, A.; White, I.N. *Biochem. Soc. Trans.*, **1991**, *19*, S127.

[9] Cerecetto, H.; González, M. *Minirev. Med. Chem.*, **2001**, *1*, 219-239.

[10] Cerecetto, H.; Di Maio, R.; González, M.; Risso, M.; Saenz, P.; Seoane, G.; Denicola, A.; Peluffo, G.; Quijano, C.; Olea-Azar, C. *J. Med. Chem.*, **1999**, *42*, 1941-1950.

[11] Olea-Azar, C.; Rigol, C.; Mendizabal, F.; Briones, R.; Cerecetto, H.; Di Maio, R.; Gonzalez, M.; Porcal, W.; Risso, M. *Spectrochimic. Acta Part A*, **2003**, *59*, 69-74.

[12] Aguirre, G.; Cerecetto, H.; Di Maio, R.; González, M.; Porcal, W., Seoane, G.; Denicola, A.; Ortega, M.A.; Aldana, I.; Monge, A. *Arch. Pharm.*, **2002**, *335*, 15-21.

[13] Olea-Azar, C.; Rigol, C.; Opazo, L.; Morello, A.; Maya, J.D.; Repetto, Y.; Aguirre, G.; Cerecetto, H.; Di Maio, R.; González, M.; Porcal, W. *J. Chil. Chem. Soc.*, **2003**, *48*, 77-79.

[14] Mallory, F.B. *Org. Synt.*, **1957**, *37*, 1-2.

[15] Cerecetto, H.; Porcal, W. *Mini Rev. Med. Chem.*, **2005**, *5*, 57-71; and references therein.

[16] Muelas-Serrano, S.; Nogal-Ruiz, J.J.; Gómez-Barrio, A. *Parasitol. Res.*, **2000**, *86*, 999-1002.

[17] Nicholson, R.; Shain, I. *Anal. Chem.*, **1964**, *36*, 706-723.

[18] Schmidt, A.; Krauth-Siegel, R.L. *Curr. Topics Med. Chem.*, **2002**, *2*, 1239-1259.

[19] (a) Maya, J.D.; Repetto, Y.; Agosin, M.; Ojeda, J.M.; Tellez, R.; Gaule, C.; Morello, A. *Mol. Biochem. Parasitol.*, **1997**, *86*, 101-106.; (b) Maya, J.D.; Morello, A.; Repetto, Y.; Rodriguez, A.; Puebla, P.; Caballero, E.; Medarde, M.; Nuñez-Vergara, L.J.; Squella, J.A.; Ortiz, M.E.; Fuentealba, J.; San Feliciano, A. *Exp. Parasitol.*, **2001**, *99*, 1-6.

[20] Risch, M.J.; Trucks, G.W.; Schlegel, H.B.; Gill, P.N.W.; Johnson, B.G.; Robb, M.A.; Cheeseman, J.R.; Keith, K.T.; Petersson, G.A.; Montgomery, J.A.; Raghavachari, K.; Al-Laham, M.A.;

Zakrzewski, V.G.; Ortiz, J.V.; Foresman, J.B.; Cioslowski, J.; Stefanov, B.B.; Nanayakkara, A.; Challacombe, M.; Peng, C.Y.; Ayala, P.Y.; Chen, W.; Wong, M.W.; Andres, J.L.; Replogle, E.S.; Gomperts, R.; Martin, R.L.; Fox, D.J.; Binkley, J.S.; Defrees, D.J.; Baker, J.; Stewart, J.P.; Head-Gordon, M.; Gonzalez, C.; Pople, J.A. Gaussian 98, Rev. A.7, Inc., Pittsburgh PA, **1998**.